

2016

## The Effect of Climate on Physiology and Immune Function in the Asian Citrus Psyllid, *Diaphorina Citri*

Grace Avecilla  
*University of Central Florida*



Part of the [Integrative Biology Commons](#)

Find similar works at: <https://stars.library.ucf.edu/honorsthesis>

University of Central Florida Libraries <http://library.ucf.edu>

This Open Access is brought to you for free and open access by the UCF Theses and Dissertations at STARS. It has been accepted for inclusion in Honors Undergraduate Theses by an authorized administrator of STARS. For more information, please contact [STARS@ucf.edu](mailto:STARS@ucf.edu).

---

### Recommended Citation

Avecilla, Grace, "The Effect of Climate on Physiology and Immune Function in the Asian Citrus Psyllid, *Diaphorina Citri*" (2016). *Honors Undergraduate Theses*. 80.

<https://stars.library.ucf.edu/honorsthesis/80>

THE EFFECT OF CLIMATE ON PHYSIOLOGY AND IMMUNE FUNCTION IN THE  
ASIAN CITRUS PSYLLID, *DIAPHORINA CITRI*

by

GRACE AVECILLA

A thesis submitted in partial fulfillment of the requirements  
for the Honors in the Major Program in Biology  
in the College of Sciences  
and in The Burnett Honors College  
at the University of Central Florida  
Orlando, Florida

Summer Term, 2016

Thesis Chair: Dr. Kenneth Fedorka

## ABSTRACT

The variation in the insect immune system is an important regulator of insect populations and the pathogens they carry. A central component of insect immunity is melanin, whose production creates cytotoxic intermediates that help to protect against a broad spectrum of pathogens. Melanin is also used in insect cuticle where it helps to improve thermoregulation and desiccation resistance, with insects having less melanized cuticles in warmer and more humid environments. Considering that cuticle melanin and immune melanin are formed by near identical biochemical pathways, they are pleiotropically linked (that is, one or more linked genes influence multiple traits). This has led to the cuticle-dependent immune investment (CDII) hypothesis, which states that adaptive responses in the cuticle can lead to non-adaptive changes in immunity and could lead to an increase in transmission of insect vectored pathogens in warming climates, due to a weaker defense against the pathogen. However, the impact of CDII on cuticle melanin and immunity, as well as infection prevalence and intensity, under seasonal conditions in the field is still unclear. In this project, we study a population of Asian citrus psyllids, *Diaphorina citri*, in the field over four seasons. *Diaphorina citri* vectors a Gram-negative bacteria, *Candidatus Liberibacter asiaticus* (CLAs), that is responsible for Huanglongbing, aka citrus greening disease, which has cost the Florida citrus industry several billion dollars. We assess pathogen load of CLAs by quantitative PCR, and assess levels of phenoloxidase activity in the insect hemolymph to measure insect immune function. We assess levels of cuticle melanin. Our results show a significant correlation between

temperature, cuticle melanin, and immune function. However, the affect of seasonality on infection prevalence and intensity remains unclear.

## **DEDICATION**

For my family, who support and love me unconditionally.

For my professors and research mentors, who teach me and embolden me to seek answers.

For my community, for Orlando, who has shown me what a compassionate, supportive community should be.

## **ACKNOWLEDGEMENTS**

I would like to thank everyone who helped make this thesis possible. Thank you to Dr. Ken Fedorka, my thesis chair, for taking me into your lab and mentoring me. Thank you to my thesis committee members, Dr. Anna Savage and Dr. Ken Teter, for your guidance and advice. Thank you to the entire Fedorka lab for helping me, encouraging me, and occasionally commiserating with me. Thank you to Louisa Collins and Sanabel Mahmoud for coming out to the field and collecting with me every month, and extra thanks to Louisa for all the field pictures. Thank you to my former research mentors, Dr. Hojun Song, Dr. Eunsoo Kim, and Dr. Aaron Heiss for mentoring me and helping shape me into a scientist. Thank you to the Office of Undergraduate Research for supporting this project. Thank you to everyone at The Burnett Honors College and the Office of Research and Community Engagement for your support.

## TABLE OF CONTENTS

INTRODUCTION .....	1
Objectives .....	4
Rational and Significance .....	5
BACKGROUND .....	6
<i>Diaphorina citri</i> biology .....	6
<i>Candidatus Liberbacter asiaticus</i> and citrus greening .....	7
Insect immunity .....	9
Melanin in the insect immune system.....	9
Cuticular melanin in insects.....	10
Cuticle melanin and climate.....	10
Cuticle dependent immune investment.....	11
APPROACH .....	15
Background.....	15
Phenoloxidase Immune Assay .....	15
Pathogen Load Assay.....	15
Cuticular Melanization Assay.....	16
Experimental Approach .....	17

Sampling .....	17
PO Immune Assay .....	17
Pathogen Load Assay.....	18
Cuticular Melanization Assay.....	19
Statistical Analysis.....	20
RESULTS .....	21
Cuticle Melanin.....	21
Abdomen Color.....	22
Phenoxidase Activity .....	22
Sex Differences.....	23
Pathogen Load .....	25
The Path Diagram .....	25
DISCUSSION.....	28
Future Studies/Amendments to approach .....	29
APPENDIX A: PATHOGEN LOAD QPCR DATA.....	31
REFERENCES .....	36



## LIST OF FIGURES

- Figure 1. General model of the cuticle-melanin and immune-melanin pathways in insects from Kutch et al. (2014). ..... 3
- Figure 2. Path diagram showing expected and possible influences under CDII. Shaded arrows represent expected influences, empty arrows represent influences that possible, but not expected. The symbols beside the each arrow represent the direction of the relationships. .... 14
- Figure 3. Example photograph from June. 1 indicates a piece of white paper, used as a standard white from month to month. 2 indicates the slide label. 3 indicates the portion of the photograph enlarged in Figure 3. 4 indicates the ruler used to find a standard length from month to month. .... 19
- Figure 4. Close up of insert from Figure 1, showing measurements for cuticular melanin. The dorsal melanin measurement, as seen on the left, is taken by creating a straight line from the tip of the head to the end of the cubitus vein on the wing, then tracing the outline of the top of the wing, pronotum, and head. The anterior triangle melanin measurement, as seen on the right, is taken by drawing a straight line from the end of the pronotum to the second leg, then tracing around the anterior-most portion of the thorax, the head and the pronotum. ImageJ takes an average grayscale value of the area within the polygon, and this measurement is used to approximate melanization. .... 20
- Figure 5. Mean anterior triangle cuticle melanization per month. A value of 0 indicates pure white and a value of 255 indicates pure black. Error bars show standard error. Months that are not significantly different from each other are marked with the same letter. 21
- Figure 6. Ratio of abdomen colors (across both sexes) by month. The width of each column represents the relative number of data points that month. .... 22
- Figure 7. Least square mean phenoloxidase activity by month. Error bars show standard error. Months that are not significantly different from each other are marked with the same letter. .... 23
- Figure 8. Least square mean body size by month. Error bars show standard error. Months that are not significantly different from each other are marked with the same letter. 24
- Figure 9. Ratio of abdomen colors (across all months) by sex. The width of each column represents the relative number of data points in each sex. .... 25

Figure 10. Regression plot of relationship between cuticle darkness and climate. Climate is estimated using principle component 1 from a principle component analysis of mean monthly temperature and maximum monthly humidity, with 10 added in order to have all positive values. Darkness is estimated principle component 1 of a principle component analysis of mean monthly dorsal melanization and mean monthly anterior triangle melanization, with 10 added in order to have all positive values. Analysis was run as a standard least squares regression, and is significant with  $p=0.0384$  and  $r=-0.6019$ . ..... 26

Figure 11. Path model diagram, with shaded arrows representing significant relationships and the empty arrow representing a relationship that is not significant. Each significant arrow is labeled with the p-value of the relationship (from GLM) and the r-value of the relationship (from SLS). ..... 27

## INTRODUCTION

Insects are an inextricable part of agricultural systems. They provide essential products and services such as pollination, but can also be highly destructive pests and vectors of disease. As a result, alterations to insect systems can have a major impact on agricultural production. This is clearly the case with the Asian citrus psyllid, *Diaphorina citri* (Order: Hemiptera, Family: Liviidae) which is an invasive insect native to Asia and first documented in Florida in the late 1990s (Grafton-Cardwell, Stelinski et al. 2013). *D. citri* vectors a Gram-negative bacteria, *Candidatus Liberbacter asiaticus* (CLas) that is responsible for citrus greening disease; a.k.a. Huanglongbing (HLB). Since their introduction, both *D. citri* and HLB have spread rapidly, costing the Florida citrus industry an estimated \$1 billion in the 2012-2013 season alone (Farnsworth, Grogan et al. 2014). A major factor that influences the spread of both the disease and its vector is the insect immune system, considering that vector immunity can influence how fitness-reducing pathogens (including vectored pathogens) are ameliorated. Therefore, it is important that we understand what drives variation in insect immune function in our changing world.

Melanin is central to insect immune function and helps protect against a wide range of pathogens, including bacteria, viruses, animals, and fungi (Gillespie, Kanost et al. 1997, Wilson, Cotter et al. 2001, Sugumaran 2002, Christensen, Li et al. 2005, Lemaitre and Hoffmann 2007). When a pathogen is identified by the immune system, hemocytes aggregate around the pathogen, and a cascade of proteases activate phenoloxidase (PO), which, along with other enzymes, converts tyrosine to melanin in a multistep pathway

(Tsakas and Marmaras 2010). However, melanin is a multifunctional pigment that plays several key physiological roles, including the darkening of insect cuticle. The thermal melanism hypothesis predicts that dark individuals will be at an advantage in cooler temperatures because they will heat faster than lighter colored individuals. In insects, several species have been shown to deposit less melanin in their cuticle in order to improve thermoregulation or avoid desiccation (Jong, Gussekloo et al. 1996, Clusella Trullas, van Wyk et al. 2007, Parkash, Sharma et al. 2008). As global temperatures rise, we have begun to see several populations of insects reduce their cuticle melanin (Brakefield and de Jong 2011, Zeuss, Brandl et al. 2014). This is important because cuticle melanin has been positively correlated with insect immune function in many insect species and there is an abundance of evidence that this is because of a pleiotropic effect, since cuticle melanin and immune melanin are formed by near identical biochemical pathways (Figure 1) (Wilson, Cotter et al. 2001, Sugumaran 2002, Bailey 2011, Fedorka, Lee et al. 2013, Fedorka, Copeland et al. 2013, Prokkola, Roff et al. 2013, Kutch, Sevgili et al. 2014). These observations have led to the cuticle-dependent immune investment hypothesis (CDII), which states that adaptive responses in the cuticle can lead to non-adaptive changes in immunity due to pleiotropy (Fedorka, Copeland et al. 2013). CDII predicts that as global temperatures rise, insects in warmer environments will display less cuticular melanin and weaker immune systems than those in cooler temperatures.

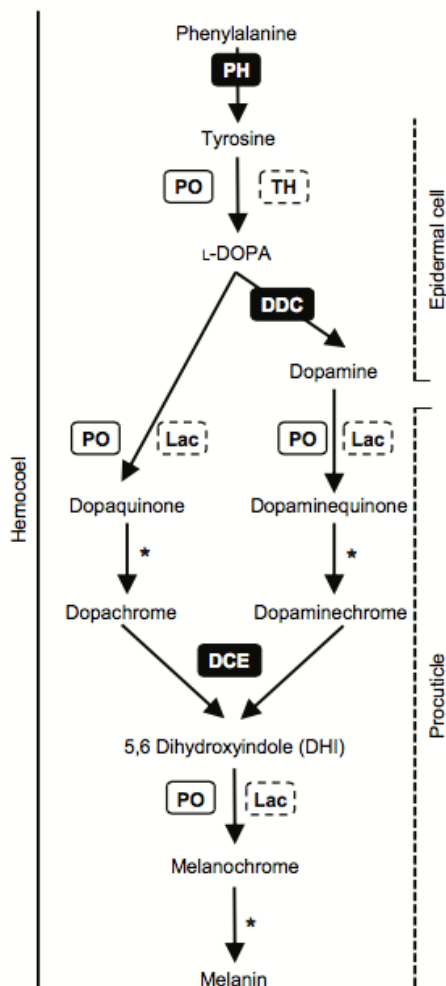


**Fig. 1. General model of the cuticle-melanin and immune-melanin pathways in insects.** Enzymes that are shared (between the pathways), cuticle-specific and immune-specific are depicted in black, dashed and white blocks, respectively. The immune-melanin pathway is generally localized to the hemocoel (solid vertical line, left side), while the cuticle-melanin pathway is localized to the epidermal cells and procuticle (dashed vertical line, right side). Asterisks depict non-enzymatic reactions. DCE, dopachrome conversion enzyme; DDC, dopadecarboxylase; Lac, laccase phenoloxidase; PH, phenylalanine hydroxylase; PO, tyrosinase phenoloxidase.

**Figure 1. General model of the cuticle-melanin and immune-melanin pathways in insects from Kutch et al. (2014).**

Recent research has found support for CDII in ground crickets (*Allonemobius socius*). Crickets from cooler northern populations or reared in the laboratory under winter-like seasonal conditions exhibited darker cuticles and higher immune function than their

counterparts from a warmer southern population or reared in the laboratory under summer-like conditions. So, seasonal or geographically distinct thermal conditions appear to adaptively shape cuticular melanin while non-adaptively shaping immune function (Fedorka, Lee et al. 2013, Fedorka, Copeland et al. 2013). A similar pattern of cuticle melanin and immune function was found in fruit flies (*Drosophila melanogaster*) that were reared under seasonal conditions in the laboratory, suggesting that TDII is a phenomenon which is conserved across the homometabolous and hemimetabolous (those insects which undergo complete and partial metamorphosis, respectively) insect clades (Kutch, Sevgili et al. 2014). However, the impact of CDII on infection prevalence and intensity under seasonal conditions in the field is still unclear. As global temperatures rise, it becomes increasingly important to understand these relationships in order to employ policies that protect out agricultural systems and allow them to prosper.

### Objectives

While there is evidence that thermal environments can directly influence insect cuticular melanin, which indirectly shapes insect immune function, the CDII hypothesis is based largely on data gathered in a laboratory setting. Furthermore, CDII has only been studied in two insect species. Therefore, in this study we aim to document the association between temperature, cuticle melanin, immune function, and infection prevalence and intensity under seasonal conditions in the field, in a third species, using an insect of agricultural importance, *D. citri*.

### Rational and Significance

The current model for insect immunity and climate change states that warming climates will increase insect immune function by increasing metabolic rates (Adamo and Lovett 2011). However, there is not much data to support this and the studies supporting this idea often fail to take into account the importance of juvenile rearing temperature, rearing their subjects in a common environment (Adamo and Lovett 2011). Insects make many decisions about their adult cuticle formation based on juvenile environment, so these studies would not have been able to detect CDII.

It is important to gather more data about the relationship between cuticular melanization and insect immunity, especially as more and more evidence appears that insects are responding to warming climates by depositing less melanin in their cuticles (Brakefield and de Jong 2011, Zeuss, Brandl et al. 2014). Studying the impact of CDII under seasonal changes in field conditions is very important, especially since hemipterans like *D. citri* are one of the most important vectors of agricultural disease.

## BACKGROUND

### *Diaphorina citri* biology

*Diaphorina citri* has a relatively broad range of host plants being able to colonize more than ten genera within the citrus family Rutaceae (Halbert and Manjunath 2004). However, because the grove we investigate in this study contains only Valencia orange *Citrus sinensis* 'Valencia', Hamlin sweet orange *Citrus sinensis* 'Hamlin', and red grapefruit *Citrus paradisi*, we will limit our range to information about interactions with those plants.

The timing of development and the duration of the lifespan of *D. citri* varies according to the literature, with estimates of lifespan ranging from 15 to 47 days, depending on temperature, season, location, host plant, and other factors (Liu and Tsai 2000, Halbert and Manjunath 2004, Alves, Diniz et al. 2014). A study conducted in Brazil of *D. citri* on Valencia orange and Hamlin sweet orange found that the average development time from egg to adult was about 17.98 and 17.75 days and the average longevity was about 31 and 29 days, respectively (Alves, Diniz et al. 2014). Though temperature for optimal development appears to be around 25-28°C, *D. citri* has been recorded surviving temperature extremes of -6°C up to 45°C (Liu and Tsai 2000, Hall, Wenninger et al. 2011).

An intriguing morphological feature of *D. citri* is its variable abdomen color. The literature refers to two or three color morphs: blue/green, orange/yellow, and grey/brown. Studies have shown that different color morphs are associated with several other characteristics, including sensitivity to various pesticides, duration of flights, reproductive patterns and output, and body mass (Wenninger, Stelinski et al. 2009, Tiwari,



Killiny et al. 2013, Martini, Hoyte et al. 2014). Furthermore, Wenniger and Hall (2008) investigated daily and seasonal changes in abdominal color in *D. citri* and found that over the lifespan of a psyllid, abdomen color varied between two, or even all three color morphs. However, the cause of the changes was not always clear. Change in abdomen color from blue/green to orange/yellow was common in females after mating, which is consistent with previous research that found an association between gravid females and orange/yellow abdomens (Halbert and Manjunath 2004), but mating is not necessarily predictive of an orange/yellow morphotype, as one third of virgin females also were observed to have an change in abdomen color from blue/green to orange/yellow (Wenninger and Hall 2008). Several studies found the blue/green morph to be more abundant than either other color morphs in both males and females all year (S. E. Halbert & Manjunath, 2004; Hall, Wenninger, & Hentz, 2011).

#### *Candidatus Liberbacter asiaticus* and citrus greening

Citrus greening disease, also known as Huanglongbing, was first documented in China in the early 20<sup>th</sup> century and has spread through Asia, and recently, into the Americas, most notably Florida and Brazil (Bové, 2006). Citrus greening is caused by the gram-negative bacteria, *Candidatus Liberbacter asiaticus* (Bové, 2006; Morgan et al., 2012). Citrus greening affects citrus plants by colonizing the phloem of plants and restricting the movement of nutrients throughout the plant, ultimately resulting in yellowed, dying leaves, and small, misshapen fruits (Bové, 2006). *Diaphorina citri* transmits *C. L. asiaticus* to citrus

plants when it feeds on the phloem of the plants, since *C. L. asiaticus* resides in the alimentary canal and salivary glands of *D. citri* (Bové, 2006; Tabachnick, 2015).

Additionally, a study by Orduño-Cruz et al. in 2016 found that *D. citri* individuals infected with *CLas* were more susceptible to infection by three different fungal pathogens, which could potentially limit their dispersal and reproductive abilities. This means that a *CLas* infection not only has a fitness effect on citrus plants, but p

*Diaphorina citri* was first found in Florida in 1998, and citrus greening disease was first detected in Florida in 2005 (Halbert, 2005). Since then, citrus greening has spread across the state and had an incredible economic impact on the citrus industry (Farnsworth, Grogan, van Bruggen, & Moss, 2014). However, the prevalence of this disease has also sparked much research into the system.

Tsai et al. (1999) conducted a study of seasonal abundance of *D. citri* in orange jasmine [*Murraya paniculata*] groves in south Florida. In the two sites they studied, *D. citri* were present year round, but varied in overall density as well as seasonal abundance. At one site, the highest density of *D. citri* occurred in October-December 1998 and August 1999, and at the other site population density peaked in May 1999 and August 1999. Both sites experienced lowest population densities between December 1998 and May 1999. Researchers found that peak population tended to coincide with new shoot flushes, and densities were correlated with weekly temperature minimums, but not weekly maximum temperatures (Tsai, Wang et al. 2002).

### Insect immunity

Insect immunity is based on innate responses, and therefore both nonspecific and available immediately upon pathogen recognition. It is broken down (somewhat subjectively, since both involve the same signaling pathways) into the humoral response and the cellular response. The products of characterized immune genes, the transcription of which results in the production of antimicrobial peptides by insect fat bodies, generally characterize the humoral response. In addition, it includes the activation of enzymatic cascades which regulate downstream immune function, including the coagulation and melanization of hemolymph (Boman & Hultmark, 1987; Gillespie, Kanost, & Trenczek, 1997). The cellular response is characterized by the action of hemocytes, which are cells that circulate freely in the hemolymph. These actions include phagocytosis of pathogens, nodulation (the creation of multicellular aggregates that trap bacteria), and encapsulation (the binding of hemocytes to larger pathogens in a multilayered capsule) (Gillespie et al., 1997). Nodulation and encapsulation both involve the eventual melanization of hemocytes surrounding the pathogen. The humoral and cellular responses are each evoked in response to specific stimuli (Tsakas and Marmaras 2010).

#### *Melanin in the insect immune system*

Insect immunity begins with pathogen recognition, which occurs by the recognition and binding of pathogen-associated molecular patterns by pattern recognition proteins. This is followed by the synthesis of antimicrobial peptides and their secretion into the hemolymph. At least two proteases must be activated before prophenolase is converted

to its active phase, phenoloxidase. Active phenoloxidase, which is sticky, is adsorbed to the pathogen where, with other enzymes, it converts tyrosine to melanin in a multistep pathway (Sugumaran 2002, Tsakas and Marmaras 2010). Melanin encapsulates pathogens and generates free radical byproducts that work to kill the pathogen (Parkash, Sharma et al. 2008). Melanin is an important and essential part of the insect immune system.

#### Cuticular melanin in insects

Melanin in insect cuticles can serve many functions, and insect cuticle melanin is shaped by both visual and non-visual selective mechanisms (True, 2003). Visual selective pressures include crypsis, aposematicism, mimicry, and sexual selection (Holloway et al., 1995; Koch, Behnecke, & French-Constant, 2000; Miller & Hollander, 2010; Siva-Jothy, 2000). Non-visual selective pressures include resistance to abrasion, UV resistance, thermoregulation, and desiccation resistance (Gunn, 1998; Hesler, Fothergill, Tindall, & Losey, 2010; Rajpurohit, Parkash, & Ramniwas, 2008). The biochemical pathway that converts tyrosine to cuticle melanin is nearly identical to the pathway that generates immune melanin (Sugumaran, 2002; True, 2003).

#### *Cuticle melanin and climate*

There is a growing body of evidence showing that as global average temperatures rise, insects are investing less melanin in their cuticles. Brakefield and de Jong (2011) investigated the frequency of melanic morphs of the two-spot ladybird beetle, *Adalia bipunctata*, along a coastal to inland cline in the Netherlands over 25 years. They found that the cline decayed drastically over that time period, from about 10% melanic morphs on the

warm coasts and 60% melanic morphs in the coolest inland climates in 1980, to a fairly uniform frequency of melanic morphs of about 20% across the sites studied in 2004. This change in frequency of melanic morphs correlated with a change in local climatic patterns, with temperature becoming more homogenous across sites and more like the warm coastal regions (Brakefield & de Jong, 2011). Similarly, Zeuss et al. (2014) investigated hundreds of species of dragonflies and butterflies in Europe, and found that between 1988 and 2006 light colored species became more prevalent and expanded their range further north. This change color was correlated with increasing annual mean temperatures (Zeuss, Brandl, Brändle, Rahbek, & Brunzel, 2014). These are just two of many examples of how global climate change is exerting a selective pressure on cuticular melanization in insect species and communities, as reviewed in Roulin (2014).

#### Cuticle dependent immune investment

Numerous studies have investigated the link between the variation in cuticle melanin and corresponding variation in immune function. There is evidence that in insect populations in laboratory settings with variations in cuticle color darker, more melanized insects have higher immune function than their lighter counterparts (Armitage & Siva-Jothy, 2005; K. M. Fedorka, Copeland, & Winterhalter, 2013; Kutch, Sevgili, Wittman, & Fedorka, 2014; Prokkola, Roff, Kärkkäinen, Krams, & Rantala, 2013). A similar pattern is found in insects with variation in levels of cuticle melanin in the field, and insects under artificial selection for darker and lighter cuticles in the lab (Armitage & Siva-Jothy, 2005; Bailey, 2011; K. Fedorka, Lee, & Winterhalter, 2013).

A commonly encountered hypothesis addressing the link between immune function and cuticle melanin is density-dependent prophylaxis. Density-dependent prophylaxis hypothesizes that insects reared in high density conditions invest more in immune function than insects reared in low density conditions, and this greater investment in immune function is often accompanied by a melanic form that is characteristic of the high density condition in many phase polyphonic insects (Barnes & Siva-Jothy, 2000; Wilson, Cotter, Reeson, & Pell, 2001). This correlation between darker morphotypes and greater immune function and pathogen resistance has been shown in a wide variety of insects, including locusts, moths, and beetles (Barnes & Siva-Jothy, 2000; Wilson et al., 2001; Wilson et al., 2002).

A link between sexually dimorphic levels of cuticle melanin and immune function has also been shown. In calopterygid damselflies, males have melanized wing patches, and variations in melanin distribution in wing patches has been shown to affect intrasexual competition and female reproductive decision making (Grether, 1996; Siva-Jothy, 1999). It has also been shown that males with more melanin in their wings are better able to clear parasite burdens. Since females prefer males with more melanin in their wings, it seems melanized wing patches are an honest indicator of male fitness (Siva-Jothy, 2000).

Recently, Ken Fedorka and colleagues have proposed cuticle-dependent immune investment (CDII) (Fedorka et al., 2013). This hypothesis states that climatic selection on cuticle melanin can indirectly shape immune function in insects (Fedorka et al., 2013; Kutch et al., 2014). This hypothesis is many ways an extension of the thermal melanism hypothesis, which states that insects will darken their cuticle in cooler environments in

order to improve thermoregulation (Trullas, van Wyk, & Spotila, 2007). This hypothesis also draws on the concept that insects will increase cuticle melanin in less humid environments to avoid desiccation. However, since cuticle melanin and immune melanin are created by nearly identical biochemical pathways, CDII presents the additional hypothesis that changes in levels of cuticle melanin will lead to change in immune function, which can be potentially non-adaptive, especially in hot climates (K. M. Fedorka et al., 2013; Kutch et al., 2014). Under CDII, as temperature and humidity, or climate, increase, insects are expected to respond by decreasing the amount of melanin in their cuticles. Because of a pleiotropic effect in melanin, immune function is predicted to positively correlate with cuticle melanin; as levels of cuticle melanin decrease, immune function will be influenced to decrease as well. Immune function directly influences pathogen load, so as immune function decreases, pathogen loads will increase. Of course, climate may directly influence immune function, immune function may directly influence cuticle melanin, and cuticle melanin may directly influence pathogen load, but biologically these would be much more complicated processes and these influences are not expected under the CDII hypothesis (Figure 2).

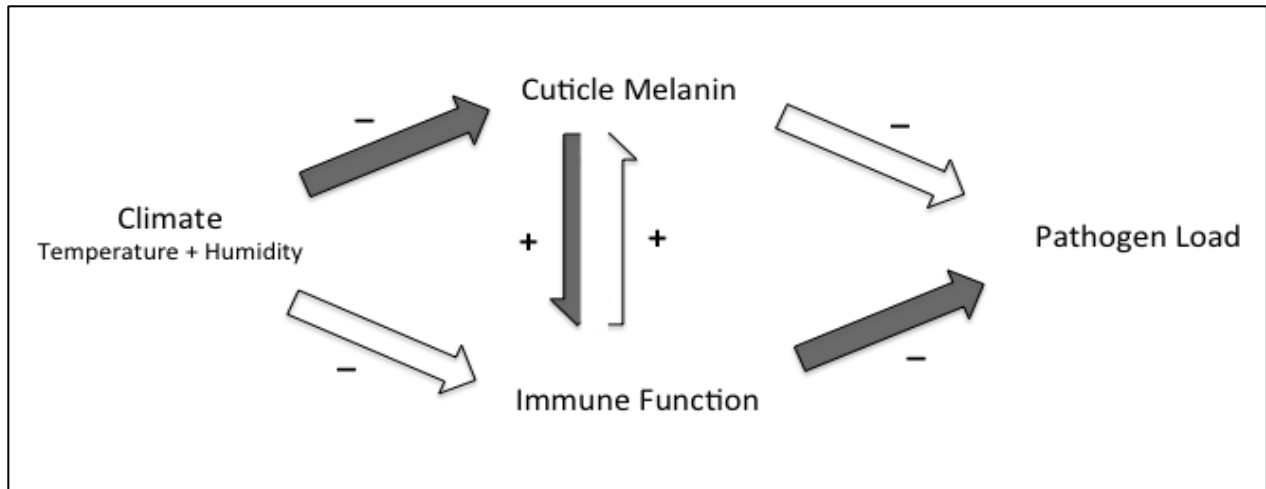


**Figure 2. Path diagram showing expected and possible influences under CDII. Shaded arrows represent expected influences, empty arrows represent influences that possible, but not expected. The symbols beside the each arrow represent the direction of the relationships.**

Evidence for CDII has been found in the ground cricket, *Allonemobius socius*, and the fruit fly, *Drosophila melanogaster*. Crickets collected from populations in North America at various latitudes were found to have more melanin and greater immune function with increasing latitude (i.e. as it became colder) (Fedorka et al., 2013). Furthermore, when reared in simulated summer and fall environments in a laboratory setting, crickets reared in a cooler fall environment had higher levels of cuticle melanin and greater immune function than their warm summer counterparts (Fedorka et al., 2013). Fruit flies reared in summer and fall environments in a laboratory setting also displayed a similar correlation between cuticular melanization and immune function (Kutch et al., 2014).



## **APPROACH**

### Background

#### *Phenoloxidase Immune Assay*

Phenoloxidase (PO) levels in insect hemolymph, and therefore the potential for phenoloxidase immune response (which leads to melanin production, as well as other immune responses), is measured by this assay. Hemolymph is obtained from the insect by puncturing the cuticle, and centrifuging the insect, so that gravity pulls the liquid hemolymph from the insect body. Hemolymph is collected in phosphate buffered saline (PBS). The enzyme  $\alpha$ -chymotrypsin is added to the hemolymph/PBS solution and the mixture is allowed to incubate, during which time  $\alpha$ -chymotrypsin cleaves and activates the pro-phenoloxidase in the hemolymph (Ohnishi, Dohke, & Ashida, 1970). After incubation, a solution of L-DOPA is added to the hemolymph solution, and the change in color as clear L-DOPA is oxidized to colored dopachrome by phenoloxidase, and the amount of color change is used to estimate phenoloxidase activity (Laughton & Siva-Jothy, 2010).

#### *Pathogen Load Assay*

Quantitative polymerase chain reaction (qPCR) is a process that quantifies levels of nucleic acids in real-time by monitoring levels of fluorescence at the end of each cycle of amplification during a polymerase chain reaction. Fluorescent dye intercalates with double-stranded DNA, so that the amount of fluorescence is directly proportional to the amount of DNA in the sample. The cycle at which fluorescence becomes detectable is called the cycle threshold (CT). The more DNA that is in the original sample, the faster the

fluorescence will increase, and the lower the CT will be. Since each PCR cycle doubles the amount of DNA in a sample, we can see the difference in abundance of different DNA targets by examining the difference in their CT values (Zipper, Brunner, Bernhagen, & Vitzthum, 2004).

Quantitative PCR allows us to estimate the abundance of bacteria in an organism using relative quantification. When we target a gene in the host and a gene in the pathogen, using genomic DNA allows us to calculate a ratio of the CT values which are used to compare approximately how many cells are in the insect body (that belong to the insect) to how many cells of the target pathogen are in the insect (Turechek 2009).

#### *Cuticular Melanization Assay*

In order to estimate cuticle melanin, we take photographs of the insects, and analyze using ImageJ software, provided by the National Institutes of Health at <http://imagej.nih.gov>), which can be used for many image processing biological measurements (Abràmoff, Magalhães, & Ram, 2004). Melanin is estimated by taking the mean grey scale darkness of pixels, with 0 being completely white and 255 being completely dark. To control for subtle differences in lighting between plates, a piece of white paper was used as a white control on each slides. To control for subtle differences between different positions on slides, a measurement of the background area of the slide was taken directly next to each insect.

## Experimental Approach

### *Sampling*

Insects were collected during the first week of every month for 12 months, from June 2015 to May 2016, from Eddy Grove, an organic orange grove in Lake County, Florida at 28.518178, -81.668592 decimal degrees (n=500 per month). Insects collected were then be randomly assigned to the PO assay, pathogen load assay, or cuticular melanization assay.

Weather data was found at Weather Underground, using the data from the weather station at Orlando International Airport. Weather measurements for each month were compiled from the weather data from the 30 days preceding each monthly collection date.

### *PO Immune Assay*

The hemolymph of 40 individuals was collected and pooled by puncturing the thorax of each individual with a fine tipped needle and centrifuging the hemolymph with 15  $\mu$ l of phosphate buffered saline (PBS) into a microcentrifuge tube (n=3). To estimate PO activity, 10  $\mu$ l from each sample was be added to a flat bottom 96 well plate, and to this 14  $\mu$ l of 0.13 mg/ml  $\alpha$ -chymotrypsin solution was added, and the samples were incubated in a cool dark place for 10 minutes. After the incubation, 90  $\mu$ l of solution of 7  $\mu$ mmol<sup>-1</sup> L-DOPA was added to each well. A microplate reader (model 680, Bio-Rad Laboratories, Hercules, CA, USA) took endpoint measurements at 0 minutes, 20 minutes, 40 minutes, 60 minutes, 80 minutes, and 100 minutes at 490  $\mu$ nm (A490). PO activity was estimated as total change in absorbance.

### *Pathogen Load Assay*

DNA was extracted from 200 individuals per month using the Qiagen DNeasy Blood and Tissue kit, combining 40 individuals in each extraction for a total of 5 extractions, each with a volume of 400  $\mu$ l. These samples were then concentrated to 25  $\mu$ l each using the Qiagen Genra Puregene Tissue Kit using the manufacturer's protocol for concentrating DNA.

Primer pairs were designed targeting actin in *D. citri* (5'-3': F-CCCTGGACTTTGAACAGGAA; R-CTCGTGGATACCGCAAGATT) and  $\beta$ -operon in *C. L. asiaticus* (5'-3': F-CGCCCCGTTTCCGTTGT; R-CAGCCTCTTTAAGCCCTAAATCAG). Both of these genes are single copy genes. Primer testing determined that each set of primers has an efficiency between 0.97 and 1.0 (with  $r^2 \geq 0.989$ ) and melt curve analyses show that only one amplicon is produced per pair.

qPCR was performed on a BioRad MyiQ Single-Color Real-Time PCR Detection System with a 96 well plate, with the profile 3 minutes at 95° C followed by 40 cycles of 15 seconds denaturation at 95° C, 30 seconds annealing at 55° C. Each assay had a total volume of 20  $\mu$ l, composed of 10  $\mu$ l SsoAdvanced™ Universal SYBR® Green Supermix, 3  $\mu$ l DNA template, 1  $\mu$ l 5  $\mu$ M forward and reverse primer mixture, and 6  $\mu$ l nuclease free water. Samples were run in duplicate and a negative control for each primer pair with nuclease-free water instead of DNA was included in each plate.

### *Cuticular Melanization Assay*

Insects were chilled at  $-80^{\circ}\text{C}$  for 10 minutes, and then digitally photographed from a lateral view using the Visionary Digital BK+ Imaging System (n=30 per month, 360 total). An example of a photograph of one of the two slides from June 2015 can be seen in Figure 2. Cuticular melanin in the anterior portion of the thorax (including the pronum) and head, as well as in the dorsal half of each individual, as seen in Figure 3, was be digitally assessed using ImageJ, which finds mean grayscale darkness of pixels within a selected area. These images were used to estimate size of individuals by the length of the tip of the head to the end of the cubitus vein in the wing, and individuals were sexed in order to estimate sex ratios in the population.



**Figure 3.** Example photograph from June. 1 indicates a piece of white paper, used as a standard white from month to month. 2 indicates the slide label. 3 indicates the portion of the photograph enlarged in Figure 3. 4 indicates the ruler used to find a standard length from month to month.



**Figure 4.** Close up of insert from Figure 1, showing measurements for cuticular melanin. The dorsal melanin measurement, as seen on the left, is taken by creating a straight line from the tip of the head to the end of the cubitus vein on the wing, then tracing the outline of the top of the wing, pronotum, and head. The anterior triangle melanin measurement, as seen on the right, is taken by drawing a straight line from the end of the pronotum to the second leg, then tracing around the anterior-most portion of the thorax, the head and the pronotum. ImageJ takes an average grayscale value of the area within the polygon, and this measurement is used to approximate melanization.

### *Statistical Analysis*

In order to create robust mean monthly measurements, we found the least square means of the raw melanization data, PO data, and qPCR, and used the least square means in our final model. Dorsal and anterior triangle melanization data were combined using a principle component analysis to create one measure (principle component one) of melanization, “darkness.” Similarly, mean temperature and maximum humidity were combined using a principle component analysis, and component one was used to create a “weather” factor.

In order to address the predictions of CDII, several multivariate ANCOVA models were created. All statistical analyses were conducted in JMP version 12.

## RESULTS

### Cuticle Melanin

Anterior triangle melanization changed significantly over the twelve-month period, ( $p < 0.0001$ ), with June, July, and August as the lightest months (Figure 4). Dorsal melanization changed significantly over time ( $p < 0.0001$ ), with a similar pattern to anterior triangle melanization, again with June, July, and August as the months with the lightest colored cuticles.

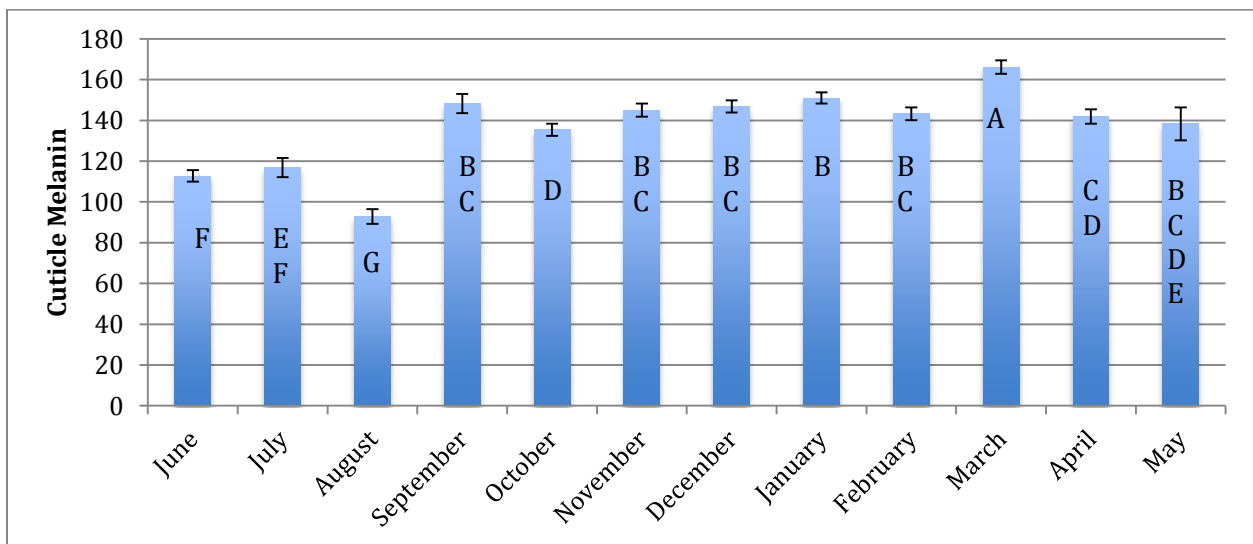


**Figure 5. Mean anterior triangle cuticle melanization per month. A value of 0 indicates pure white and a value of 255 indicates pure black. Error bars show standard error. Months that are not significantly different from each other are marked with the same letter.**

The 'darkness' component accounted for 94.6% of variation in mean melanization. A principle component analysis of the adjacent plate color was created using adjacent dorsal and adjacent triangle measurements. Principle component one accounted for 98.8% of variation in plate color, and was saved. As expected from the results of analysis of anterior triangle and dorsal melanization, darkness changed significantly over time ( $p < 0.0001$ ),

with June, July, and August as the lightest months. All of these models were run with white values and adjacent plate color as covariates with month.

### Abdomen Color

The frequency of each abdomen color morph observed differs across the months, with light red/orange abdomens only in the majority in March (Figure 6). However, this analysis was limited because a large amount of psyllids from June 2015-December 2015 were of unknown sex and therefore excluded from this analysis.

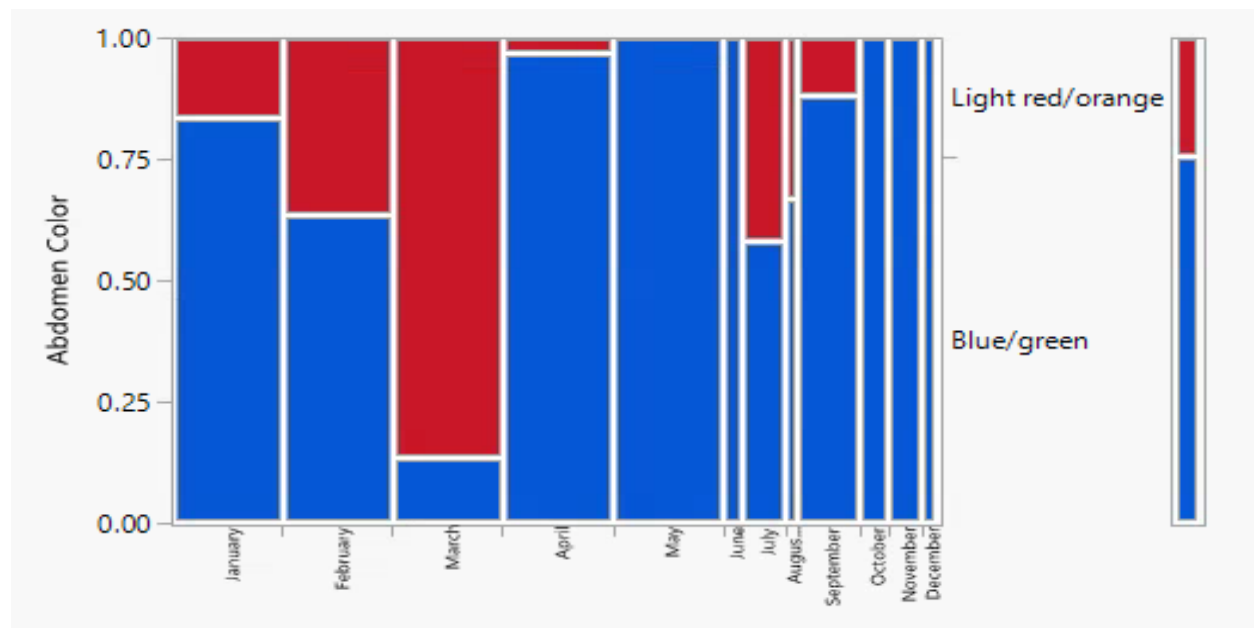


**Figure 6. Ratio of abdomen colors (across both sexes) by month. The width of each column represents the relative number of data points that month.**

### Phenoloxidase Activity

Mean phenoloxidase activity differed significantly from month to month ( $p=0.0002$ ), in the eight months that for which there is data (Figure 7). March had the highest level of



PO activity. This model was run with combined/uncombined samples as a covariant with month.

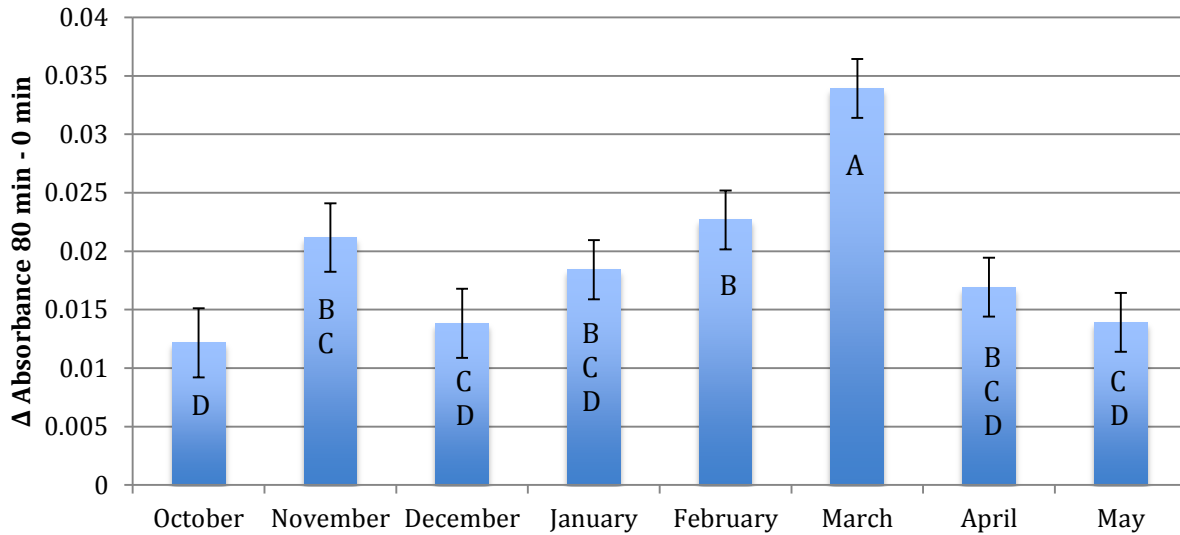


**Figure 7. Least square mean phenoloxidase activity by month. Error bars show standard error. Months that are not significantly different from each other are marked with the same letter.**

#### Sex Differences

As reported in previous studies, sex significant predictor of body size ( $p < 0.0001$ ) and month significant predictor of body size ( $p < 0.0001$ ) with females slighter larger than males (on average 2.99mm and 2.90mm respectively). Furthermore, the warmer months tended to produce smaller individuals than cooler months (Figure 8).

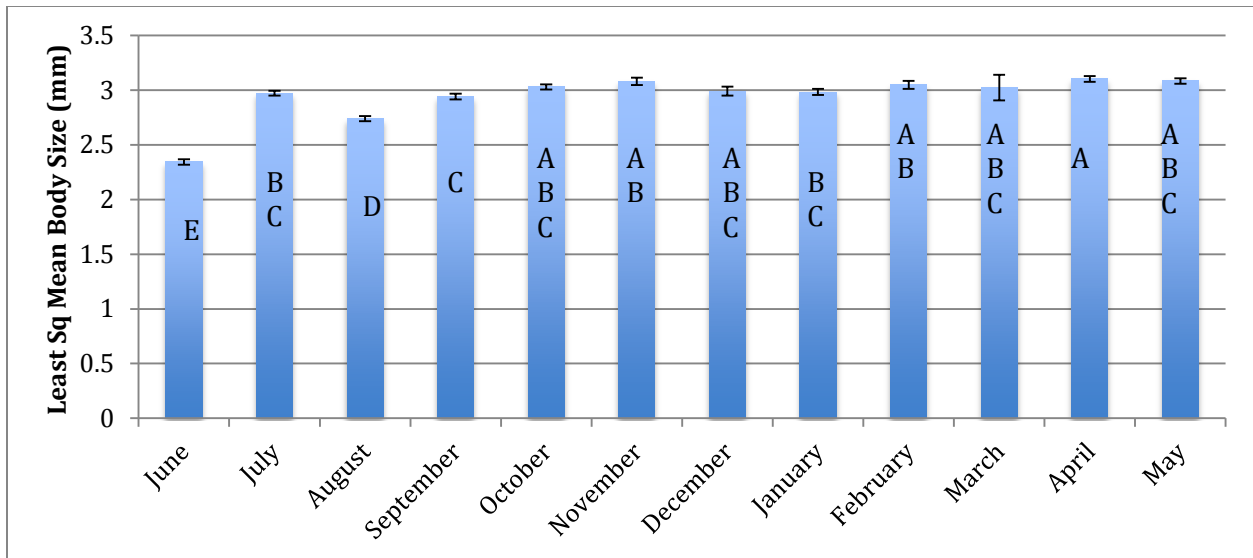


**Figure 8. Least square mean body size by month. Error bars show standard error. Months that are not significantly different from each other are marked with the same letter.**

When controlling for month (in the model  $\text{melanin} = \text{month} + \text{sex} + \text{white} + \text{adjacent plate color}$ ), sex does not significantly influence the amount of cuticle melanin in either the dorsal or the anterior triangle ( $p=0.3331$  and  $0.1106$ , respectively).

Sexes differed in abdomen color when all observed data points were tested (Figure 9). The relative frequency of each abdomen color in each sex did not remain stable from month to month either. However, this analysis was limited because a large amount of psyllids from June 2015-December 2015 were of unknown sex and therefore excluded from this analysis.

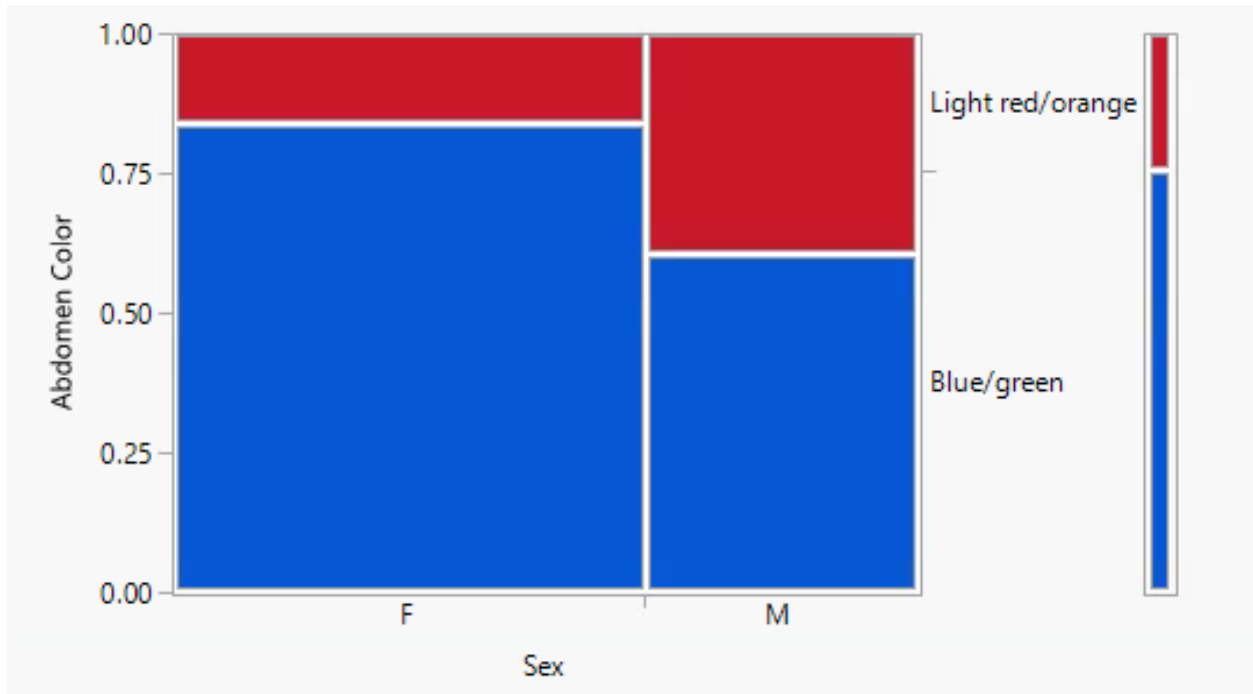


**Figure 9. Ratio of abdomen colors (across all months) by sex. The width of each column represents the relative number of data points in each sex.**

### Pathogen Load

Neither pathogen presence nor pathogen load intensity were significantly correlated with month. There were very few degrees of freedom for this test, due to limited and unusable data (see Appendix A for pathogen load qPCR data).

### The Path Diagram

Since temperature and humidity were our two predictive climatic factors, we combined them into a single factor called 'climate' using a principle component analysis of mean temperature and maximum humidity. Maximum humidity was used instead of mean humidity because it had a more significant association with melanin measurements in an

overall screening of relationships between all variables. Principle component one, which was used to create the climate factor, accounted for 95 % of variation.

Mean monthly darkness was estimated using the least square mean from the following model: darkness PC1= month + white + adjacent color PC1. When run in a least squares model with climate as a predictor variable, there was a significant negative relationship between darkness and climate ( $p=0.0384$ ,  $r=-0.6019$ ), as seen in Figure 4.

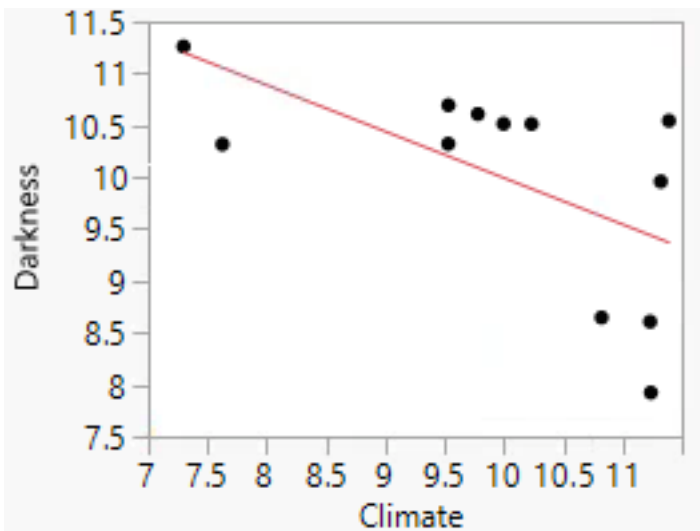


**Figure 10. Regression plot of relationship between cuticle darkness and climate. Climate is estimated using principle component 1 from a principle component analysis of mean monthly temperature and maximum monthly humidity, with 10 added in order to have all positive values. Darkness is estimated principle component 1 of a principle component analysis of mean monthly dorsal melanization and mean monthly anterior triangle melanization, with 10 added in order to have all positive values. Analysis was run as a standard least squares regression, and is significant with  $p=0.0384$  and  $r=-0.6019$ .**

When reconstructing our path diagram, we used anterior triangle as a measurement of melanization as it was the most significant of the three melanin measurements (dorsal, anterior triangle, and darkness). The models were tested as Generalized Linear Models with normal distributions, but the r-values were generated using a Standard Least Squares Model.

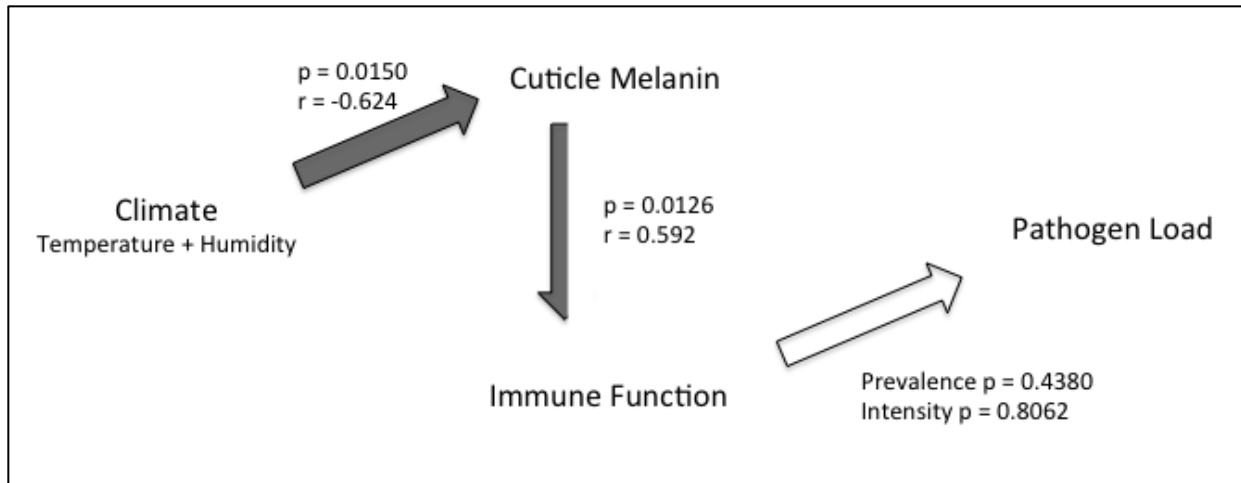


Figure 11. Path model diagram, with shaded arrows representing significant relationships and the empty arrow representing a relationship that is not significant. Each significant arrow is labeled with the p-value of the relationship (from GLM) and the r-value of the relationship (from SLS).

## DISCUSSION

This study is incredibly important because it verifies that the predictions made by CDII can be seen not only in a laboratory setting, but in the field, under true seasonal conditions, in a non-model insect as well. We see a significant relationship between temperature and humidity, cuticle melanin, and immune function in *D. citri* in the field, and the relationships exist as CDII predicts: as temperature and humidity increase, cuticle melanin decreases, and immune function decreases. However, while we do see this pattern, we were unable to obtain the last portion in this study, that is the relationship between an immune parameter (in this case PO activity), and pathogen prevalence and intensity. Still, we believe that this is not necessarily because the relationship does not exist, but because our data were not robust. The lack of sound gene data and how to remedy that issue is addressed in the following section.

Since CDII is seen in these field experiments, then this hypothesis has the potential to be applied to many more important systems in agriculture and human health (Harwood & James, 1979; Ng & Falk, 2006). Some potential systems for future study include insects that are beneficial to agriculture but are susceptible to virulent pathogens, such as the honey bee, *Apis mellifera*, and insects that vector pathogens that cause disease in humans, such as the *Anopheles* mosquito, which transmits the organism that causes malaria.

### Future Studies/Amendments to approach

During the course of this study, several amendments were made to the experimental approach. The initial PO protocol, which originally used 1.3 mg/ml  $\alpha$ -chymotrypsin and had 20 minute incubation, yielded no results. We hypothesized that the lack of response was due to using too high of a concentration of  $\alpha$ -chymotrypsin and too long an incubation period (which had been optimized for *D. melanogaster*, rather than *D. citri*), resulting in off-target enzymatic activity. After some trials, we found that 0.13 mg/ml  $\alpha$ -chymotrypsin and a 10 minute incubation yielded results. However, because we had limited samples and some were already used in the higher concentration/incubation version of the assay, some samples had to be combined to create 10  $\mu$ l hemolymph samples. Samples that were combined are marked with -c in the data set, and the potential influence of combined versus non-combined hemolymph samples was accounted for statistically.

The DNA extraction protocol was also amended. In December 2015, we ran June-December samples using the qPCR protocol. These samples had variable responses, with several samples not working at all. After some investigation, we believed that this could be because of the high variability in the concentration of the DNA extractions (some were very high; many were very low). In order to increase concentrations and decrease the variability between concentrations, we increased the number of psyllids in each DNA extraction from 3 psyllids to 20 psyllids. We found that generally, this did increase the concentration of the DNA extractions, but there was still a lot of variation in concentration between samples. Data in this thesis comes from June-December extractions with 3 psyllids per extraction and January-May extractions with 20 psyllids per extraction. We are currently testing

various other extraction methods to find a DNA extraction method that maximizes DNA concentration and minimizes variance between samples.

Future qPCR work on this study will be done using TaqMan qPCR chemistry. Probe based qPCR has greater specificity than SYBR® Green chemistry, because the use of probes ensures that even if there is off-target amplification, only the target gene will fluoresce. Furthermore, TaqMan probe based qPCR has been shown to detect *C. L. asiaticus* with increased sensitivity (Morgan et al., 2012). We will use primer pairs and probes that have been used in previously published papers targeting *C. L. asiaticus* (Morgan et al., 2012) and *D. citri* (Ammar, Shatters, Lynch, & Hall, 2011).

This study will be continued for another year by another researcher in the Fedorka Lab in order to obtain as robust a data set as possible, and the data presented here will be combined with the new data.



## **APPENDIX A: PATHOGEN LOAD QPCR DATA**

The following table displays qPCR pathogen load data. Table displays sample name, the month the sample was collected, the plate number of the qPCR run, the sample's left-most position on the plate, the mean cycle threshold of the duplicate runs for the *D. citri* target gene, the mean cycle threshold of the duplicate runs for the *CLas* target gene, and the difference in cycle threshold number between the two genes. A cycle threshold shown for the *CLas* gene indicates presence of the pathogen. Intensity of infection is calculated by the difference in CT values. When using SYBR chemistry, CT values over 30 are usually discarded as artifact. Samples in which there was a great discrepancy between duplicate CT values or which produced no CT values are labeled in the table as "NO DATA."

Sample	Month	Plate	Position	ACP mean CT	Clas mean CT	$\Delta(\text{ACP-Clas CT})$
5-Jun	June	1	A1	34.53	NO DATA	NO DATA
5-Jul	July	1	B1	23.065	NO DATA	NO DATA
5-Aug	August	1	C1	30.4	NO DATA	NO DATA
5-Sep	September	1	D1	NO DATA	NO DATA	NO DATA
5-Oct	October	1	E1	25.96	NO DATA	NO DATA
5-Nov	November	1	F1	NO DATA	NO DATA	NO DATA
5-Dec	December	1	G1	22.55	NO DATA	NO DATA
1-Jan	January	1	H1	20.9	32.045	11.145
1-Feb	February	1	A5	29.78	NO DATA	NO DATA
1-Mar	March	1	B5	NO DATA	NO DATA	NO DATA
1-Apr	April	1	C5	20.915	NO DATA	NO DATA
1-May	May	1	D5	18.125	38.32	20.195
6-Jun	June	1	E5	20.94	33.755	12.815
6-Jul	July	1	F5	21.2	NO DATA	NO DATA
6-Aug	August	1	G5	36.6	20.79	-15.81
6-Sep	September	1	H5	NO DATA	NO DATA	NO DATA
6-Oct	October	1	C9	25.8	NO DATA	NO DATA
6-Nov	November	1	D9	NO DATA	NO DATA	NO DATA
6-Dec	December	1	E9	22.545	NO DATA	NO DATA

2-Jan	January	1	F9	19.49	24.265	4.775
2-Feb	February	1	G9	21.295	NO DATA	NO DATA
2-Mar	March	1	H9	NO DATA	2.15	NO DATA
2-Apr	April	2	A1	32.86	37.13	4.27
2-May	May	2	B1	22.18	24.64	2.46
7-Jun	June	2	C1	23.795	21.605	-2.19
7-Jul	July	2	D1	NO DATA	20.78	NO DATA
7-Aug	August	2	E1	NO DATA	19.38	NO DATA
7-Sep	September	2	F1	NO DATA	20	NO DATA
7-Oct	October	2	G1	NO DATA	27.96	NO DATA
7-Nov	November	2	H1	NO DATA	21.93	NO DATA
7-Dec	December	2	A5	NO DATA	NO DATA	NO DATA
3-Jan	January	2	B5	26.135	27.36	1.225
3-Feb	February	2	C5	22.83	26.03	3.2
3-Mar	March	2	D5	21.17	26.88	5.71
3-Apr	April	2	E5	19.01	27.575	8.565
3-May	May	2	F5	21.71	26.055	4.345
8-Jun	June	2	G5	29.17	22.6	-6.57
8-Jul	July	2	H5	22.06	NO DATA	NO DATA
8-Aug	August	2	E9	31.67	23.7	-7.97
4-Jan	January	2	F9	30.84	23.17	-7.67
4-Feb	February	2	G9	36.58	29.405	-7.175
4-Mar	March	2	H9	NO DATA	NO DATA	NO DATA
8-Sep	September	3	A1	38.1	NO DATA	NO DATA
8-Oct	October	3	B1	22.585	NO DATA	NO DATA
8-Nov	November	3	C1	NO DATA	NO DATA	NO DATA
8-Dec	December	3	D1	24.49	NO DATA	NO DATA
4-Apr	April	3	E1	16.795	30.525	13.73
4-May	May	3	F1	NO DATA	38.27	NO DATA
9-Jun	June	3	G1	NO DATA	NO DATA	NO DATA
9-Jul	July	3	H1	22.81	31.145	8.335
9-Aug	August	3	A5	35.49	NO DATA	NO DATA
9-Sep	September	3	B5	31.205	NO DATA	NO DATA
9-Oct	October	3	C5	26.57	NO DATA	NO DATA
9-Nov	November	3	D5	34.97	NO DATA	NO DATA
13-Dec	December	3	E5	NO DATA	34.39	NO DATA
5-Jan	January	3	F5	16.83	23.825	6.995
5-Feb	February	3	G5	16.68	26.38	9.7
5-Mar	March	3	H5	32.26	38.51	6.25
5-Apr	April	3	E9	17.535	28.46	10.925

5-May	May	3	F9	20.31	NO DATA	NO DATA
10-Jun	June	3	G9	26.3	NO DATA	NO DATA
10-Jul	July	3	H9	19.615	33.17	13.555
10-Aug	August	4	A1	34.435	NO DATA	NO DATA
10-Sep	September	4	B1	32.055	NO DATA	NO DATA
10-Oct	October	4	C1	NO DATA	NO DATA	NO DATA
10-Nov	November	4	D1	36.19	NO DATA	NO DATA
10-Dec	December	4	E1	25.815	NO DATA	NO DATA
6-Jan	January	4	F1	22.36	NO DATA	NO DATA
6-Feb	February	4	G1	29.765	NO DATA	NO DATA
6-Mar	March	4	H1	23.49	27.08	3.59
6-Apr	April	4	A5	23.92	NO DATA	NO DATA
6-May	May	4	B5	22.215	29.67	7.455
7-Mar	March	4	C5	20.885	24.915	4.03
11-Sep	September	4	D5	2.78	NO DATA	NO DATA
11-Nov	November	4	E5	21.995	NO DATA	NO DATA
7-Apr	April	4	F5	23.495	36.77	13.275
11-Jul	July	4	G5	35.71	NO DATA	NO DATA
11-Aug	August	4	H5	22.465	32.795	10.33
11-Dec	December	4	D9	NO DATA	NO DATA	NO DATA
12-Sep	September	4	E9	NO DATA	NO DATA	NO DATA
11-Oct	October	4	F9	NO DATA	NO DATA	NO DATA
12-Nov	November	4	G9	NO DATA	NO DATA	NO DATA
13-Nov	November	5	A1	NO DATA	NO DATA	NO DATA
1-Nov	November	5	B1	NO DATA	NO DATA	NO DATA
2-Nov	November	5	C1	35.14	NO DATA	NO DATA
3-Nov	November	5	D1	NO DATA	NO DATA	NO DATA
1-Dec	December	5	E1	29.785	NO DATA	NO DATA
12-Dec	December	5	F1	NO DATA	NO DATA	NO DATA
12-Oct	October	5	G1	NO DATA	NO DATA	NO DATA
13-Oct	October	5	H1	30.25	NO DATA	NO DATA
11-Jun	June	5	A5	NO DATA	NO DATA	NO DATA
12-Jul	July	5	B5	33.62	NO DATA	NO DATA
1-Aug	August	5	C5	22.925	36.595	13.67
2-Aug	August	5	D5	25.895	35.72	9.825
3-Aug	August	5	E5	24.51	NO DATA	NO DATA
7-May	May	5	F5	20.35	NO DATA	NO DATA
1-Sep	September	5	G5	33.46	NO DATA	NO DATA
2-Sep	September	5	H5	25.15	NO DATA	NO DATA
3-Sep	September	5	D9	21.58	NO DATA	NO DATA

4-Sep	September	5	E9	22.2	NO DATA	NO DATA
13-Sep	September	5	F9	NO DATA	NO DATA	NO DATA

## REFERENCES

- Abràmoff, M. D., Magalhães, P. J., & Ram, S. J. (2004). Image processing with ImageJ. *Biophotonics international*, 11(7), 36-42.
- Ammar, E.-D., Shatters, R. G., Lynch, C., & Hall, D. G. (2011). Detection and relative titer of *Candidatus Liberibacter asiaticus* in the salivary glands and alimentary canal of *Diaphorina citri* (Hemiptera: Psyllidae) vector of citrus huanglongbing disease. *Annals of the Entomological Society of America*, 104(3), 526-533.
- Armitage, S. A. O., & Siva-Jothy, M. (2005). Immune function responds to selection for cuticular colour in *Tenebrio molitor*. *Heredity (Edinb)*, 94(6), 650-656.
- Bailey, N. W. (2011). A test of the relationship between cuticular melanism and immune function in wild-caught Mormon crickets. *Physiological Entomology*, 36(2), 155-164. doi:10.1111/j.1365-3032.2011.00782.x
- Barnes, A. I., & Siva-Jothy, M. T. (2000). Density-dependent prophylaxis in the mealworm beetle *Tenebrio molitor* L. (Coleoptera: Tenebrionidae): cuticular melanization is an indicator of investment in immunity. *Proceedings of the Royal Society of London B: Biological Sciences*, 267(1439), 177-182. doi:10.1098/rspb.2000.0984
- Boman, H. G., & Hultmark, D. (1987). Cell-Free Immunity in Insects. *Annual Review of Microbiology*, 41(1), 103-126. doi:doi:10.1146/annurev.mi.41.100187.000535
- Bové, J. M. (2006). Huanglongbing: a destructive, newly-emerging, century-old disease of citrus. *Journal of plant pathology*, 7-37.
- Brakefield, P. M., & de Jong, P. W. (2011). A steep cline in ladybird melanism has decayed over 25 years: a genetic response to climate change? *Heredity (Edinb)*, 107(6), 574-578. doi:10.1038/hdy.2011.49
- Farnsworth, D., Grogan, K. A., van Bruggen, A. H., & Moss, C. B. (2014). The Potential Economic Cost and Response to Greening in Florida Citrus. *Choices*, 29(3).
- Fedorka, K., Lee, V., & Winterhalter, W. (2013). Thermal environment shapes cuticle melanism and melanin-based immunity in the ground cricket *Allonemobius socius*. *Evolutionary Ecology*, 27(3), 521-531. doi:10.1007/s10682-012-9620-0
- Fedorka, K. M., Copeland, E. K., & Winterhalter, W. E. (2013). Seasonality influences cuticle melanization and immune defense in a cricket: support for a temperature-dependent immune investment hypothesis in insects. *J Exp Biol*, 216(Pt 21), 4005-4010. doi:10.1242/jeb.091538
- Gillespie, J. P., Kanost, M. R., & Trenczek, T. (1997). Biological mediators of insect immunity. *Annual Review of Entomology*, 42, 611-643.
- Grether, G. F. (1996). Sexual selection and survival selection on wing coloration and body size in the rubyspot damselfly *Hetaerina americana*. *Evolution*, 1939-1948.
- Gunn, A. (1998). The determination of larval phase coloration in the African armyworm, *Spodoptera exempta* and its consequences for thermoregulation and protection from UV light. *Entomologia Experimentalis et Applicata*, 86(2), 125-133. doi:10.1046/j.1570-7458.1998.00273.x

- Halbert, S. (2005). *The discovery of huanglongbing in Florida*. Paper presented at the Proceedings of the 2nd International Citrus Canker and Huanglongbing Research Workshop.
- Halbert, S. E., & Manjunath, K. L. (2004). Asian citrus psyllids (Sternorrhyncha: Psyllidae) and greening disease of citrus: a literature review and assessment of risk in Florida. *Florida Entomologist*, *87*(3), 330-353.
- Hall, D. G., Wenninger, E. J., & Hentz, M. G. (2011). Temperature studies with the Asian citrus psyllid, *Diaphorina citri*: Cold hardiness and temperature thresholds for oviposition. *Journal of Insect Science*, *11*(1), 83.
- Harwood, R. F., & James, M. T. (1979). *Entomology in human and animal health*: Bailliere Tindall.
- Hesler, L. S., Fothergill, K., Tindall, K. V., & Losey, J. E. (2010). Variation in Elytral Macular Forms of *Coccinella septempunctata* L. (Coleoptera: Coccinellidae) in North America. *Proceedings of the Entomological Society of Washington*, *112*(4), 500-507. doi:10.4289/0013-8797.112.4.500
- Holloway, G. J., Brakefield, P. M., Jong, P. W. D., Ottenheim, M. M., Vos, H. D., Kesbeke, F., & Peynenburg, L. (1995). A Quantitative Genetic Analysis of an Aposematic Colour Pattern and Its Ecological Implications. *Philosophical Transactions of the Royal Society B: Biological Sciences*, *348*(1326), 373-379. doi:10.1098/rstb.1995.0075
- Koch, P. B., Behnecke, B., & French-Constant, R. H. (2000). The molecular basis of melanism and mimicry in a swallowtail butterfly. *Current Biology*, *10*(10), 591-594. doi:10.1016/S0960-9822(00)00494-2
- Kutch, I. C., Sevgili, H., Wittman, T., & Fedorka, K. M. (2014). Thermoregulatory strategy may shape immune investment in *Drosophila melanogaster*. *J Exp Biol*, *217*(Pt 20), 3664-3669. doi:10.1242/jeb.106294
- Laughton, A. M., & Siva-Jothy, M. T. (2010). A standardised protocol for measuring phenoloxidase and prophenoloxidase in the honey bee, *Apis mellifera*. *Apidologie*.
- Miller, C. W., & Hollander, S. D. (2010). Predation on heliconia bugs, *Leptoscelis tricolor*: examining the influences of crypsis and predator color preferences. *Canadian Journal of Zoology*, *88*(1), 122-128. doi:10.1139/Z09-128
- Morgan, J. K., Zhou, L., Li, W., Shatters, R. G., Keremane, M., & Duan, Y.-P. (2012). Improved real-time PCR detection of 'Candidatus Liberibacter asiaticus' from citrus and psyllid hosts by targeting the intragenic tandem-repeats of its prophage genes. *Molecular and Cellular Probes*, *26*(2), 90-98. doi:<http://dx.doi.org/10.1016/j.mcp.2011.12.001>
- Ng, J. C., & Falk, B. W. (2006). Virus-vector interactions mediating nonpersistent and semipersistent transmission of plant viruses. *Annu Rev Phytopathol*, *44*, 183-212. doi:10.1146/annurev.phyto.44.070505.143325
- Ohnishi, E., Dohke, K., & Ashida, M. (1970). Activation of prephenoloxidase. *Archives of Biochemistry and Biophysics*, *139*(1), 143-148. doi:[http://dx.doi.org/10.1016/0003-9861\(70\)90055-X](http://dx.doi.org/10.1016/0003-9861(70)90055-X)
- Prokcola, J., Roff, D., Kärkkäinen, T., Krams, I., & Rantala, M. J. (2013). Genetic and phenotypic relationships between immune defense, melanism and life-history traits

- at different temperatures and sexes in *Tenebrio molitor*. *Heredity (Edinb)*, 111(2), 89-96. doi:10.1038/hdy.2013.20
- Rajpurohit, S., Parkash, R., & Ramniwas, S. (2008). Body melanization and its adaptive role in thermoregulation and tolerance against desiccating conditions in drosophilids. *Entomological Research*, 38(1), 49-60. doi:10.1111/j.1748-5967.2008.00129.x
- Roulin, A. (2014). Melanin-based colour polymorphism responding to climate change. *Glob Chang Biol*, 20(11), 3344-3350. doi:10.1111/gcb.12594
- Siva-Jothy, M. (1999). Male wing pigmentation may affect reproductive success via female choice in a calopterygid damselfly (Zygoptera). *Behaviour*, 136(10), 1365-1377.
- Siva-Jothy, M. T. (2000). A mechanistic link between parasite resistance and expression of a sexually selected trait in a damselfly. *Proceedings of the Royal Society of London B: Biological Sciences*, 267(1461), 2523-2527. doi:10.1098/rspb.2000.1315
- Sugumaran, M. (2002). Comparative Biochemistry of Eumelanogenesis and the Protective Roles of Phenoloxidase and Melanin in Insects. *Pigment Cell Research*, 15(1), 2-9. doi:10.1034/j.1600-0749.2002.00056.x
- Tabachnick, W. J. (2015). *Diaphorina citri (Hemiptera: Liviidae) Vector Competence for the Citrus Greening Pathogen 'Candidatus Liberibacter Asiaticus'*.
- True, J. R. (2003). Insect melanism: the molecules matter. *Trends in Ecology & Evolution*, 18(12), 640-647. doi:<http://dx.doi.org/10.1016/j.tree.2003.09.006>
- Trullas, S. C., van Wyk, J. H., & Spotila, J. R. (2007). Thermal melanism in ectotherms. *Journal of Thermal Biology*, 32(5), 235-245.
- Wilson, K., Cotter, S. C., Reeson, A. F., & Pell, J. K. (2001). Melanism and disease resistance in insects. *Ecology Letters*, 4(6), 637-649. doi:10.1046/j.1461-0248.2001.00279.x
- Wilson, K., Thomas, M. B., Blanford, S., Doggett, M., Simpson, S. J., & Moore, S. L. (2002). Coping with crowds: density-dependent disease resistance in desert locusts. *Proceedings of the National Academy of Sciences*, 99(8), 5471-5475.
- Zeuss, D., Brandl, R., Brändle, M., Rahbek, C., & Brunzel, S. (2014). Global warming favours light-coloured insects in Europe. *Nat Commun*, 5. doi:10.1038/ncomms4874
- Zipper, H., Brunner, H., Bernhagen, J., & Vitzthum, F. (2004). Investigations on DNA intercalation and surface binding by SYBR Green I, its structure determination and methodological implications. *Nucleic acids research*, 32(12), e103-e103.